Am J Physiol Gastrointest Liver Physiol 285: G938–G948, 2003.
First published July 3, 2003; 10.1152/ajpgi.00470.2002.

Fundamental role of ClC-3 in volume-sensitive Cl^- channel function and cell volume regulation in AGS cells

Nan Ge Jin,[1] Jin Kyoung Kim,[2] Dong Ki Yang,[1] Soo Jin Cho,[3] Jung Mogg Kim,[3] Eun Ju Koh,[4] Hyun Chae Jung,[4] Insuk So,[1] and Ki Whan Kim[1]

[1]*Department of Physiology and Biophysics, Seoul National University College of Medicine, Seoul 110-799;* [2]*Department of Anesthesiology, Sungkyunkwan University School of Medicine, Suwon 440-746;* [3]*Department of Microbiology and Institute of Biomedical Science, Hanyang University College of Medicine, Seoul 33-791;* [4]*Department of Internal Medicine, Liver Research Institute, Seoul National University College of Medicine, Seoul, Korea 110-744*

Submitted 29 October 2002; accepted in final form 26 June 2003

Jin, Nan Ge, Jin Kyoung Kim, Dong Ki Yang, Soo Jin Cho, Jung Mogg Kim, Eun Ju Koh, Hyun Chae Jung, Insuk So, and Ki Whan Kim. Fundamental role of ClC-3 in volume-sensitive Cl^- channel function and cell volume regulation in AGS cells. *Am J Physiol Gastrointest Liver Physiol* 285: G938–G948, 2003. First published July 3, 2003; 10.1152/ajpgi.00470.2002.—Volume regulation is essential for cell function, but it is unknown which channels are involved in a regulatory volume decrease (RVD) in human gastric epithelial cells. Exposure to a hypotonic solution caused the increase in AGS cell volume, followed by the activation of a current. The reversal potential of the swelling-induced current suggested that Cl^- was the primary charge carrier. The selectivity sequence for different anions was $I^- > Br^- > Cl^- > F^-$ > gluconate. This current was inhibited by flufenamate, DIDS, tamoxifen, and 5-nitro-2-(3-phenylpropylamino)benzoate. Intracellular dialysis of three different anti-ClC-3 antibodies abolished or attenuated the Cl^- current and disrupted RVD, whereas the current and RVD was unaltered by anti-ClC-2 antibody. Immunoblot studies demonstrated the presence of ClC-3 protein in Hela and AGS cells. RT-PCR analysis detected expression of ClC-3, MDR-1, and pICln mRNA in AGS cells. These results suggest a fundamental role of endogenous ClC-3 in the swelling-activated Cl^- channels function and cell volume regulation in human gastric epithelial cells.

swelling-activated chloride current; anti-ClC-3; gastric epithelial cell

MAINTENANCE OF A CONSTANT cell volume in the face of fluctuating intra- and extracellular osmolarity is essential for normal cell function (14, 26). Our previous studies (30) showed that volume-sensitive Cl^- current ($I_{Cl,vol}$) was present in gastric myocytes and participated in regulatory volume decrease (RVD). However, it is still unknown which channels are involved in RVD in human gastric epithelial cells after exposure to hypotonic solutions.

In recent years, several proteins have been described as possible molecular candidates for volume-sensitive chloride currents. Paulmichl et al. (18) sequenced pICln and suggested that it might be a possible candidate for a chloride channel. However, it could be shown that pICln is localized mainly in the cytosol and that its protein structure is not that of a typical channel. Instead it was suggested that pICln is a regulator for a volume-sensitive chloride channel (13). P-glycoprotein (P-gp), the product of the multidrug resistance (MDR1) gene, proposed as a candidate for the swelling-activated chloride channels, was subsequently shown to be a regulator of endogenous channel activity (2, 24, 25). Another swelling-activated chloride channel expressed in many cell types, ClC-2, has also been suggested as contributing to RVD (29). However, controversies regarding several key aspects of the regulation of swelling-activated chloride channels need to be resolved (1, 7, 11).

Subsequently, the role of ClC-3 in swelling-activated chloride channels has been challenged. When expressed in NIH/3T3 cells, ClC-3 gave rise to a basally active chloride conductance with similar biophysical and pharmacological characteristics as native volume-sensitive anion channels (5). Furthermore, ClC-3 antisense treatment delayed the rate of activation of native volume-sensitive anion channels and reduced its amplitude in a dose-dependent manner (27). In addition, a polyclonal anti-ClC-3 antibody (Ab) was shown to functionally inhibit native volume-sensitive anion channels in guinea pig cardiac cells, canine pulmonary arterial smooth muscle cells, and *Xenopus laevis* oocytes (5). But the ClC-3 hypothesis as a volume-sensitive chloride channel has recently become controversial (15, 21, 22, 28). Availability of a specific experimental tool to inhibit endogenous ClC-3 function would be very useful and may help to resolve some of the existing controversies in this field. In the present report, we used three different anti-ClC-3 antibodies to eliminate endogenous ClC-3 function and demonstrate that ClC-3 may be the fundamental molecular entity responsible for volume-sensitive chloride channels and RVD in human gastric epithelial cells.

Address for reprint requests and other correspondence: I. So, Dept. of Physiology and Biophysics, Seoul National Univ. College of Medicine, 28 Yongon-Dong, Chongro-Gu, Seoul, Korea 110-799 (E-mail address: insuk@plaza.snu.ac.kr).

The costs of publication of this article were defrayed in part by the payment of page charges. The article must therefore be hereby marked "*advertisement*" in accordance with 18 U.S.C. Section 1734 solely to indicate this fact.

EXPERIMENTAL PROCEDURES

Cells. AGS human gastric epithelial cells (CRL 1739; American Type Culture Collection, Manassas, VA) were grown in 90% Ham's F-12 medium (GIBCO-BRL) supplemented with 10% FBS and 20 μg/ml gentamicin in an atmosphere of 5% CO_2 at 37°C. For electrophysiological experiments, the cells were subcultured in petri dishes (COSTAR) and used after 3–4 days.

Electrophysiological recordings. Experiments were performed at room temperature (22–25°C) by using the whole cell configuration of the patch-clamp technique. The chamber was continuously perfused throughout the experiment. Patch-clamp pipettes were manufactured from borosilicate glass capillaries (GC 150T-7.5; Harvard Apparatus) by using a two-stage puller (Narishige, Tokyo, Japan) and fire-polished to give final resistances of 2–5 MΩ when filled with pipette solution. The bath was grounded via an agar bridge. Whole cell currents were recorded with an Axopatch 200A amplifier and pCLAMP 6.01 software (Axon Instruments). Junction potentials were measured by changing the external solution from the same pipette solution to normal sodium chloride concentration solution ($[Cl^-]_o$ = 86 mM; see *Solutions and chemicals*) and to solutions of lower $[Cl^-]_o$ (46 and 16 mM). The mean junction potential changes were −0.4 ± 0.2, 3.2 ± 0.4, and 7.3 ± 0.7 mV, respectively.

Measurement of single-cell diameter. The diameter of a single epithelial cell was measured under whole cell voltage-clamp conditions. The microscope used in this experiment was a Diaphot TMD (Nikon, Japan). Transmitted light was reflected by a full mirror, images of the cells were projected onto a charge-coupled device camera (model C3077; Hamamatsu, Japan), and were then stored by using a video tape recorder. For each image, the video camera provided two interleaved frames (odd and even) at a rate of 25/s. With the aid of Digital Vision version 4.0 software (Cyclope-Digital Vision), the captured images were used for cell diameter measurement.

Data analysis. For the majority of experiments, voltage pulses of 800-ms duration were applied in 20-mV steps to levels between −120 mV and +80 mV, from a holding potential of −60 mV. The percent effect of a drug for the indicated voltage step was determined as follows: $[(I_{hypo} - I_{iso}) - (I_{hypo+drug} - I_{iso})]/(I_{hypo} - I_{iso}) \times 100$.

Reversal potentials (E_{rev}) were determined from current-voltage (*I-V*) relationships measured by using 1,000-ms voltage ramps from −80 mV to +80 mV or from +100 mV to −100 mV. Data were expressed as means ± SE. The number of observations is designated by *n*. Statistical analysis was done by Student's paired and unpaired *t*-tests; a value of $P < 0.05$ was considered to be statistically significant.

Solutions and chemicals. The isotonic bath solution contained (in mM) 80 NaCl (or TEA-Cl), 2 $CaCl_2$, 1 $MgCl_2$, 10 Hepes, 10 glucose, buffered to pH 7.4 with NaOH. The osmolarity was adjusted to 300 mosM with sucrose. The hypotonic bath solution was obtained by reducing the sucrose concentration, which gave an osmolarity of 250 mosM. In the experiments to test the anion selectivity, 80 mM NaCl of the hypotonic bath solution was replaced by the same concentration (in 80 mM) of NaI, NaBr, NaF, or sodium gluconate. The osmolarity was adjusted to 250 mosM by using sucrose. In the measurements in which bath solutions contained different chloride concentrations or in which Na were replaced by *N*-methyl-D-glutamine (NMDG), all potentials were corrected for liquid junction potentials. The standard pipette CsCl solution contained (in mM) 130 CsCl, 10 HEPES, 0.1 (1 or 10) EGTA, 3 MgATP, 0.5 GTP, and was buffered at pH 7.2 with CsOH. The osmolarity was 275–285 mosM. Osmolarity of all solutions was measured with the Vapor Pressure Osmometer (Wescor). The test drugs DIDS, tamoxifen, flufenamic acid, and 5-nitro-2-(3-phenylpropylamino)benzoate (NPPB) were purchased from Sigma (St. Louis, MO).

Western blot analysis. Confluent epithelial monolayers in six-well plates were washed with ice-cold PBS, and lysed in a 0.5 ml/well lysis buffer (150 mM NaCl, 20 mM Tris, pH 7.5, 0.1% Triton X-100, 1 mM PMSF, 10 mg/ml aprotonin). The lysates were sonicated for 5 s on ice and centrifuged at 12,000 *g* for 20 min. Protein concentrations in the lysates were determined by the Bradford method (Bio-Rad, Hercules, CA) by using bovine serum albumin (Sigma) as a standard. Fifteen milligrams of protein per lane were size fractionated on a denaturing, nonreducing, 6% polyacrylamide minigel (Mini-PROTEIN II; Bio-Rad) and electrophoretically transferred to a nitrocellulose membrane (0.1-mm pore size). ClC-2 was detected by using rat anti-ClC-2 Ab (Alomone Labs). ClC-3 was detected by using rabbit anti-ClC-3 Ab (Alomone Labs) or goat anti-ClC-3 Ab (Santa Cruz Biotechnology, Santa Cruz, CA) as a primary Ab, and peroxidase-conjugated anti-rabbit or anti-goat IgG (Transduction Laboratories, Lexington, KY) as a secondary Ab. Specifically bound peroxidase was detected by enhanced chemiluminescence (Amersham Life Science, Piscataway, NJ) and exposure to X-ray film (model XAR5; Eastman Kodak, Rochester, NY) for 10 to 30 s (12). Inhibition assay was performed that purified ClC-3 protein (3 μg; Alomone Labs) was reacted with primary Ab (9 μg, Alomone Labs) at RT for 1 h before the addition of primary Ab to nitrocellulose membrane.

Antibodies of anti-ClC-2 and anti-ClC-3. For the intracellular dialysis experiments in human gastric epithelial cells, anti-ClC-2 Ab, and anti-ClC-3 Ab (Alomone Labs) were diluted in deionized water and added into the pipette solution (final concentration of 7.5 μg/ml). For preabsorbed anti-ClC-2 Ab and anti-ClC-3 Ab, Ab and antigen were dissolved separately, mixed in a weight ratio of 1:10, stored in the refrigerator overnight, and added to the pipette solution to achieve a final concentration of Ab and antigen of 7.5 and 75 μg/ml, respectively. The osmolarity of the pipette dialysis solutions was not significantly altered by inclusion of either Ab alone or preabsorbed Ab.

Due to recent concerns (22) regarding the specificity of this Ab, another commercial anti-ClC-3 Ab (Santa Cruz Biotechnology) was used for Western blotting and added into the pipette solution to achieve a final concentration of 30 μg/ml. In addition, a new rabbit polyclonal affinity-purified anti-ClC-3 Ab (a gift from Dr. Joseph R. Hume) raised against a different COOH terminus epitope (amino acids 670–687 of the mouse sequence). The peptide used to generate the $C_{670-687}$ Ab is similar to the ClC-3 epitope previously used to generate a specific COOH terminus anti-ClC-3 Ab, which exhibited no cross reactivity with human ClC-1, rat ClC-2, or human ClC-4 (10).

RT-PCR. Total RNA was extracted from human gastric epithelial cells by using a RNeasy Mini Kit (Qiagen, Hilden, Germany) following the procedures of the manufacture. First-strand cDNA was synthesized from the RNA preparations with the SuperScript Preamplification System (GIBCO-BRL, Manassas, VA). In brief, RNA samples were reverse transcribed at 42°C for 50 min by incubation with 20 μl of a RT mixture containing the following constituents (in mM): 20 Tris·HCl (pH 8.4), 50 KCl, 2.5 $MgCl_2$, 1 each 2-deoxynucleotide 5′-triphosphate, 10 DTT, 100 μg random hexamer, and 200 units of SuperScript II RT. The RT was then inactivated by heating at 70°C for 15 min. The resultant first-strand cDNA was used for the PCR procedure. PCR was performed

in a total volume of 50 μl of a buffer solution containing (in mM) 60 Tris·HCl (pH 8.5), 15 $(NH_4)_2SO_4$, 1.5 $MgCl_2$, 0.2 2-deoxynucleotide 5′-triphosphate, and 250 units of Taq (Bioneer, Korea). The sets of primers for ClC-3 (GenBank accession no. AF172729), MDR-1 (GenBank accession no. AF016535) and pICln (GenBank accession no. AU117367) were predicted to yield 540-bp, 600-bp, and 726-bp product, respectively. The optimum temperature cycling protocol was determined to be 94°C for 1 min, 52°C for 1 min, and 72°C for 2 min for two rounds of 40 cycles by using a programmable thermal cycler (GeneAmp PCR System 2400; Perkin-Elmer). Two sets of negative control experiments were performed by including primers but no cDNA or by including primers with RNA that had not been reverse transcribed (no RT added). PCR products were cloned into pGEM-T Easy vector (Promega, Madison, WI) and subjected to sequencing by using an ABI PRISM 310 automated sequencer (Perkin-Elmer).

Primer design. Primers were designed with the aid of the designer program Primer3 at http://www-genome.wi.mit.edu/cgi-bin/primer/primer3.cgi by using the corresponding rat mRNA sequences. The specificity of the primers for the target gene was checked against the databases by using Fasta3 at http://www2.ebi.ac.uk/fasta3/ and primers were checked for hairpin loops and palindromes by using the Cybergene Utility at http://www.cybergene.se/primer.html. The oligonucleotides were synthesized by Genosys, Cambridge, UK. The primers designed and used are listed in Table 1.

RESULTS

Biophysical characterization. Human gastric epithelial cells were voltage clamped in the whole cell configuration and held at −60 mV with CsCl solution in the pipette. Applying hyposmotic NaCl solution (250 mosM) slowly activated a sustained current at a holding potential of −60 mV, as shown in Fig. 1*A*. To investigate the role of the sustained current in the volume regulation of gastric epithelial cells under hyposmotic condition, the trace current was shown in Fig. 1*A* where repetitive voltage ramp pulses (from +100 mV to −100 mV, −0.2 V/s) were applied from a holding potential of −60 mV every 20 s. Simultaneously, a change in cell diameter was measured by using the video image analysis system. The change in cell volume indicated as the relative diameter [the cell diameter under hypotonic solutions (D_{hypo}) is divided by that under isotonic solutions (D_{iso})] was obvious through the microscope and was followed by a current activation. The discernible activation of currents occurred ~3 min (3.0 ± 0.8 min, n = 8) after the exchange of bath solution. The increased current and increased cell diameter were reversed slowly on returning to the isosmotic solutions (300 mosM), indicating that the current was volume dependent. The activation of current variably reached its steady state ~11 min (11.4 ± 0.9 min, n = 8) after the discernible change of holding current. A second exposure to a hypotonic solution reactivated the current. *I-V* relationship was shown in Fig. 1*B*. Employing voltage-clamp step pulses (800 ms) from −120 mV to +80 mV showed this current started to inactivate at positive potentials more than +40 mV (Fig. 1*C*). The extent of current inactivation gradually increased with depolarization and was quite variable in different cells.

To isolate and study swelling-activated Cl^- current ($I_{Cl,swell}$), we prepared isotonic and hypotonic TEA external solutions in which all of the Na^+ was replaced with TEA. Exposure to the TEA hypotonic solution triggered the development of a current that had no significant difference from that to NaCl hypotonic solution (data not shown). The Cl^- nature of the current was also apparent from the close proximity of its E_{rev} to the theoretical equilibrium potential for Cl^-. When $[Cl^-]_o$ was reduced from 86 to 46 and 16 mM by replacement with sodium gluconate, the amplitude of the outward current was decreased, whereas the inward current was not significantly changed (Fig. 2*A*). The E_{rev} was shifted in the positive direction by decreasing $[Cl^-]_o$, i.e., 10.6 ± 1.3 mV, 22.6 ± 2.5 mV, and 38.8 ± 2.8 mV at 86, 46, and 16 mM $[Cl^-]_o$, respectively (filled squares in the inset of Fig. 2*B*, n = 6). This result suggests that the hyposmotic-swelling-activated current was induced by the activation of an anion channel permeable to Cl^-. However, at each value of $[Cl^-]_o$, E_{rev} did not exactly correspond to the E_{Cl} calculated

Table 1. *Primers designed and used in the RT-PCR*

Primer Sequence	Nucleotide Sequence Number	Expected Size
CIC3		
forward 5′-GATGGCTAGTAGTAACAC	384–400	540 bp (ECORI site at 719)
TAACAGGATTGGCATCAG-′3	401–418	
reverse 5′-GCACCTCCCTTTTTTTAGC	923–940	
AGCTGAGGCAGCTGATA-′3	941–958	
MDR-1		
forward 5′-CAGTAGCTGAAGAGGTC	873–890	600 bp (ECORI site at 1174)
TTGGCAGCAATTAGAACT-′3	891–908	
reverse 5′-AATATCCTGTCCATCAAC	1473–1490	
CCTTACATTTATGGTCCT-′3	1491–1508	
pICln		
forward 5′-TTGCCGCACTCTGCTGCT GGAATTCCATGAGCTTCC TCAAAAGT-′3	−18 from ATG cloning sequence added before ATG cloning sequence added after TGA +11 from TGA	726 bp
reverse 5′-GCTCTAGAGCTCAGTGAT CAACATCTGC ATAAATCATTTTCAGTGA-′3		

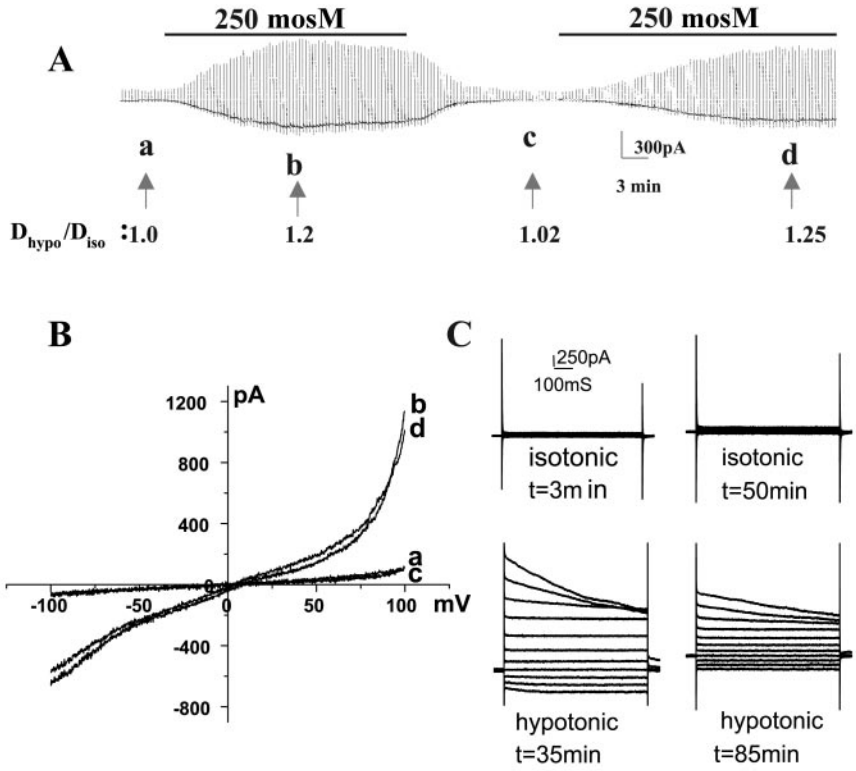

Fig. 1. Current activation on osmotic cell swelling under whole cell recordings in single gastric epithelial cells. *A*: membrane potential was held at −60 mV and ramp pulses (from +100 to −100 mV, $dV/dt = -0.20$ V/s) were applied repetitively every 20 s. Cell diameter was measured simultaneously and given under the membrane current trace. Hyposmotic stimulation slowly increased cell diameter and was followed by the activation of a current. Visible swelling always started ~15 s before the onset of current activation. *B*: current-voltage (*I-V*) relationships obtained from voltage ramp protocols at different times as indicated in *A* (*a–d*). *C*: whole cell currents in response to voltage pulses, to levels from −120 to +80 mV in 20 mV steps. D_{hypo}, hypotonic solution; D_{iso}, isotonic solution.

from the Nernst equation ($E_{Cl} = RT/F$ In $[Cl]_i/[Cl]_o$, i.e., 10.6, 26.7, and 53.8 mV for respective concentrations, open circles in the inset of Fig. 2*B*), where $[Cl]_i$ is intracellular Cl concentration and $[Cl]_o$ is extracellular Cl concentration. There is the possibility that replacement of extracellular Cl^- results in a decrease in the intracellular Cl^- activity, especially after activation of chloride current (I_{Cl}) that is inward at the holding potential. This might also shift the actual Nernst potentials to values that are less depolarized than would be calculated from the known values of $[Cl^-]$. However, the difference is also likely to be due to a significant permeability to gluconate, which is used as the substitute for Cl^- in this experiment. As can be seen in Fig. 3, gluconate can pass through the anion channel and the relative permeability was calculated to be 0.20 compared with that of Cl^-. Considering the permeability of gluconate, the expected E_{rev} could be recalculated by using the Goldman-Hodgkin-Katz equation $\{E_{Cl} = RT/F \text{ In } (P_{Cl}[Cl]_i + P_{gluconate}[gluconate]_i)/(P_{Cl}[Cl]_o + P_{gluconate}[gluconate]_o)\}$ and the results are 10.6, 22.6, and 37.8 mV, respectively (open triangles in the inset of Fig. 2*B*). These values correspond well with the measured values of E_{rev} for the osmotic swelling-induced current in this experiment. The above results suggest that this outwardly rectifying current in gastric epithelial cells is mostly due to the chloride current activated by hyposmotic cell swelling (i.e., I_{Cl}). Figure 2 shows the current traces from a typical cell (*A*), and the *I-V* relationship (*B*) obtained by voltage ramp protocols at different conditions as indicated in Fig. 2*A* (*a–c*). The chord conductance measured at +100 mV is 18.5 ± 1.6, 12.8 ± 0.9, and 6.9 ± 0.1 nS at 86, 46, and 16 mM $[Cl^-]_o$, respectively ($n = 3$). In addition, when we replaced 80, 40, and 10 mM Na with NMDG, the E_{rev} did not change (data not shown), suggesting that no significant Na^+ currents occurred under hypotonic condition.

To determine whether this Cl^- current activation could be modulated by intracellular Ca^{2+}, we conducted a series of recordings in human gastric epithelia cells dialyzed with intracellular solutions in which EGTA was raised from 0.1 to 1 or 10 mM without an influence on the characteristics of this current ($n = 5$), suggesting that Ca^{2+} is not involved in its activation (data not shown).

To examine the Cl^- dependence and the anion selectivity of the channel, Cl^- in the hypotonic solution was replaced by I^-, Br^-, F^-, or gluconate (each 80 mM). Voltage ramps between +100 and −100 mV for 1,000 ms were applied in the presence of the different extracellular anions (Fig. 3). The anion selectivity of the channel was examined with the cells in hyposmotic bathing solutions in which Cl^- ions were replaced with other anionic species. The current and voltage relations were obtained with a voltage-ramp protocol between +100 mV and −100 mV (−0.20 V/s). Figure 3 shows a representative *I-V* relationship of volume-sensitive anion currents when extracellular Cl^- was subsequently replaced with the same concentration of I^-, Br^-, F^-, or gluconate. From the *I-V* curves obtained at maximal current activation, the E_{rev} values were evaluated. Ion permeabilities relative to those of Cl^- ions were calculated from E_{rev} values by using the

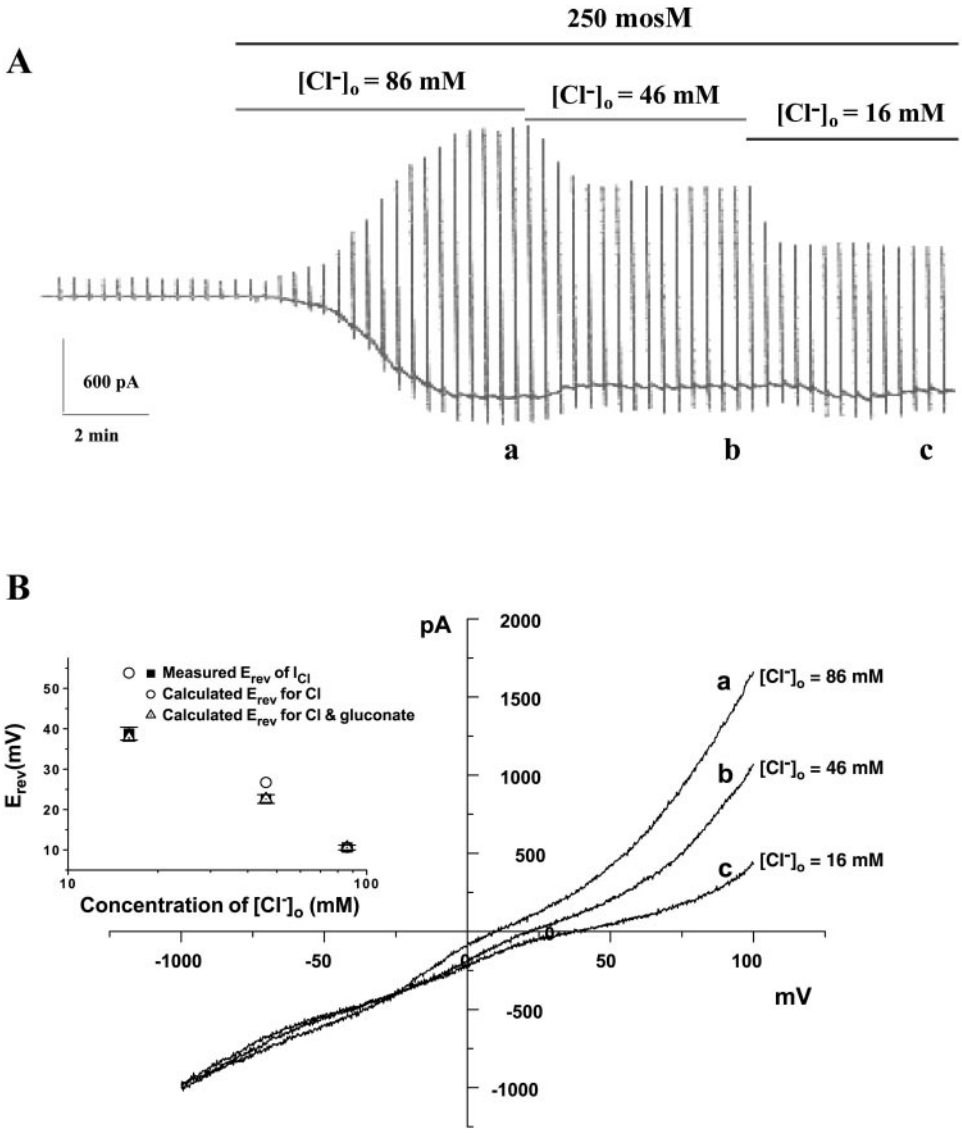

Fig. 2. Effect of the changes in extracellular Cl^- concentrations ($[Cl^-]_o$) on the swelling-activated current. *A*: current activation on osmotic cell swelling was measured at $[Cl^-]_o$ of 86, 46, and 16 mM, respectively. *B*: *I-V* relationships of hyposmotic swelling-activated current at various $[Cl^-]_o$, as indicated in *A* (*a–c*). The reversal potentials (E_{rev}) of the swelling-induced inward currents were shifted by changes of chloride concentrations. *Inset* shows the relationship between measured E_{rev} and E_{rev} calculated according to the Nernst equation and Goldman-Hodgkin-Katz equation.

Goldman-Hodgkin-Katz equation under bionic conditions ($E_{rev} = RT/F \ln P_{Cl} [Cl]_i/P_x[X]_o$), assuming that the currents were carried solely by anions and that the $[Cl^-]_i$ would not change during the perfusion of hyposmotic solution (Table 2). P_x is the permeability of anions other than chloride, and $[X]_o$ is the concentration of extracellular anions other than chloride. The sequence of relative permeability obtained was $I^- > Br^- > Cl^- > F^- >$ gluconate.

Pharmacological characterization. To characterize the type of chloride current present in the human gastric epithelial cells, we investigated the effects of the chloride transport blockers DIDS (100 μM), Cl^- channel blockers flufenamate (100 μM), antioestrogen tamoxifen (10 μM), and NPPB (100 μM). Applying the ramp with an applied pulse from −80 to + 80 mV ($dV/dt = 0.16$ V/s), DIDS suppressed the current (Fig. 4*A*) in a voltage-dependent manner; the outward current was significantly more susceptible to DIDS compared with the inward current ($P < 0.01$, $n = 7$, Fig. 4). The outward current at +40 mV was inhibited by

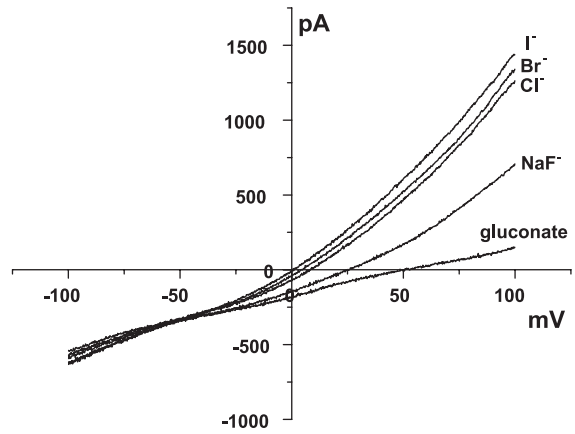

Fig. 3. Effect of extracellular anion substitution on the *I-V* of volume-sensitive currents measured by a voltage ramp stimulus. A voltage ramp from +100 to −100 mV was applied after the steady current activation was observed in osmotically swollen single AGS cells. Cells were superfused with hyposmotic medium in which NaCl was replaced with the sodium salt of the anions indicated.

Table 2. *Effects of Cl^- ion replacement on reversal potentials of volume-sensitive anion current*

Anion	V_{rev}* (mV)	P_X/P_{Cl}	*n*
Gluconate	53.3 ± 2.8	0.20	13
F^-	24.5 ± 1.7	0.62	11
Cl^-	10.4 ± 1.2	1.00	19
Br^-	3.5 ± 1.0	1.41	9
I^-	−3.0 ± 1.1	1.81	13

V_{rev} values were obtained from current-voltage relationship plots as indicated in MATERIALS AND METHODS. Relative anion permeabilities (P_x/P_{Cl}) were calculated using the Goldman-Hodgkin-Katz equation. *Corrected for junction potentials (around +8 mV for gluconate and +3 mV for NaF but < 1 mV for other anions).

91.8 ± 2.5%, but inward current at −80 mV was suppressed only by 37.8 ± 10.8% in the presence of DIDS. Flufenamate and tamoxifen also inhibited the current, but affected both outward and inward currents. In the presence of flufenamate (Fig. 4*B*), outward current at +40 mV and inward current at −80 mV were suppressed by 81.6 ± 8.6 and 77.2 ± 10.1%, respectively ($P < 0.01$, $n = 6$). In the presence of tamoxifen (Fig. 4*C*), outward current at +40 mV and inward current at −80 mV was suppressed by 96.8 ± 1.5 and 91.8 ± 1.9% ($P < 0.01$, $n = 14$). The effect NPPB on the volume regulation of gastric epithelial cells was studied under hyposmotic conditions. The trace current is shown in Fig. 5*A*, where repetitive voltage ramp pulses (from +100 to −100 mV, −0.2 V/s) were applied from a holding potential of −60 mV every 20 s. Simultaneously, a change in cell diameter (D_{hypo}/D_{iso}, the cell diameter under hypotonic solutions is divided by that under isotonic solutions) was measured by using the video image analysis system. In this cell, the amplitude of I_{Cl} was suppressed by NPPB, whereas the cell diameter was enhanced from 18 to 28% by the same treatment. The current and voltage relationships were shown in Fig. 5*B*. Averaged inhibitory effects of NPPB on I_{Cl} at +100 mV (by 92.8 ± 1.8%, $n = 5$) and at −100 mV (92.4 ± 1.5%, $n = 5$) were compared in Fig. 5*C*.

Ab experiments. Figure 6*A* illustrates the effects of intracellular dialysis of either 7.5 μg/ml ClC-2 Ab or 7.5 μg/ml ClC-3 Ab on the Cl^- current activated by exposure to hypotonic solutions at a holding potential of −60 mV. After 5 min of intracellular dialysis with ClC-3 Ab, the Cl^- current activated by hypotonic bath solutions was inhibited ($n = 4$, $P < 0.01$) and RVD was disrupted (data not shown). In contrast, the properties of the Cl^- current in the cells dialyzed with ClC-2 Ab

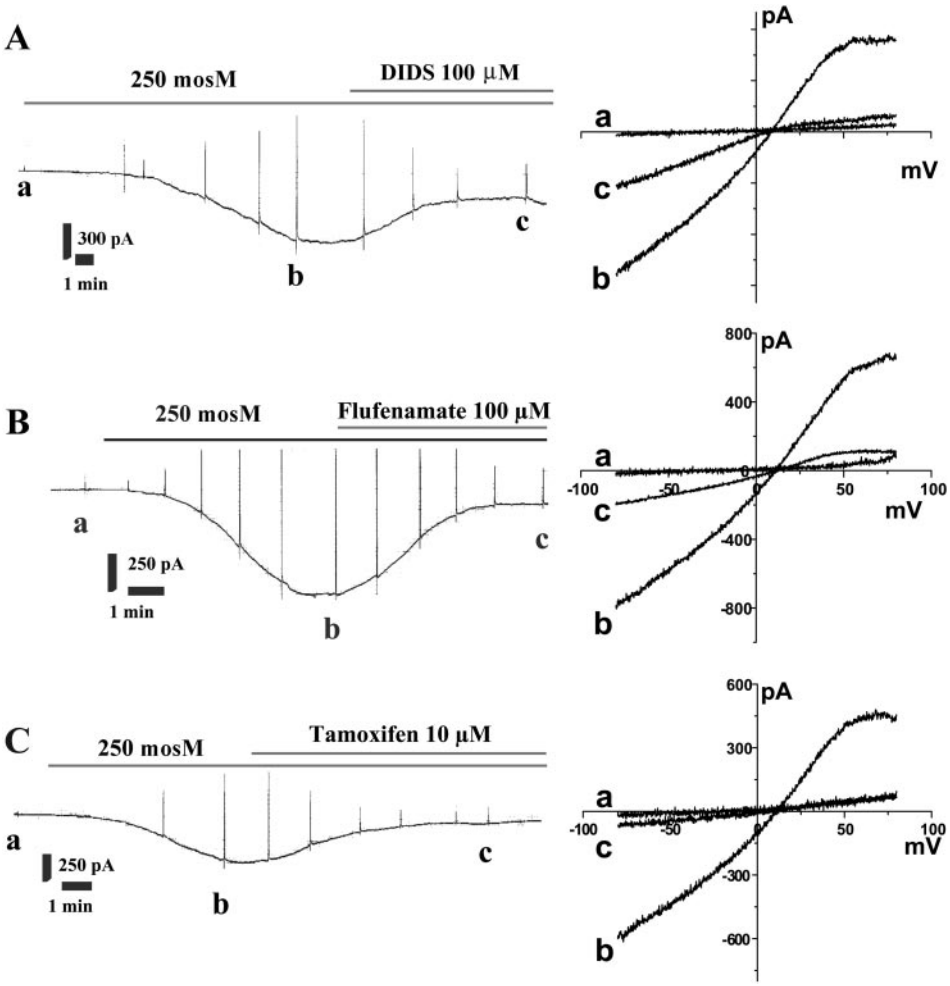

Fig. 4. Effects of DIDS (*A*), flufenamic acid (*B*), and tamoxifen (*C*) on the swelling-activated Cl^- current. *Left*, representative whole cell currents. *Right*, *I-V* obtained at *left a*, *b*, and *c* from applying ramp pulse from −80 to +80 mV.

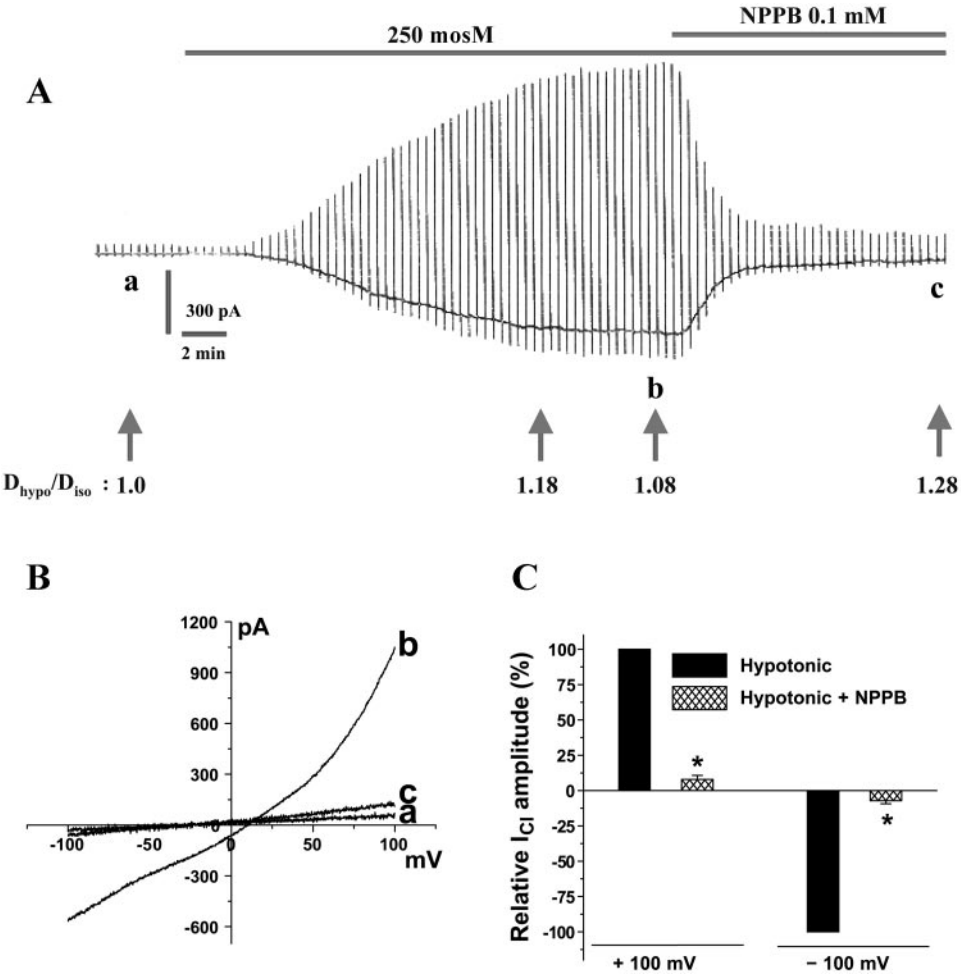

Fig. 5. Effects of 5-nitro-2-(3-phenylpropylamino)benzoate (NPPB) on volume-sensitive Cl^- current and cell diameter. *A*: simultaneous measurement of cell diameter and membrane current in the absence and presence of NPPB. Membrane potential was held at −60 mV and ramp pulses (from +100 to −100 mV, $dV/dt = -0.20$ V/s) were applied repetitively every 20 s. Relative cell diameter was given under the membrane current trace. NPPB was administrated after the steady current activation was observed under hypotonic solutions. *B*: *I-V* relationships obtained from voltage ramp protocols at different times as indicated in *A* (*a*–*c*). *C*: averaged effects of NPPB on volume-sensitive Cl^- currents at +100 and −100 mV are compared. *Significant difference ($P < 0.01$, $n = 5$).

($n = 4$), appeared remarkably unaffected and similar to those observed in the cells dialyzed with antigen-preabsorbed ClC-2 Ab or antigen-preabsorbed ClC-3 Ab, whereas the process of RVD was unaltered (data not shown). To observe the specificity of anti-ClC-2 Ab (Alomone Labs), Western blot analysis was used. Positive control (ClC-2 antigen, 10 ng) was detected, whereas ClC-2 was not found ($n = 5$). An actin band corresponding to ~45 kDa, was detected with anti-actin Ab, suggesting that the proteins were intact in Western blot analysis. These results indicate that ClC-2 is not present in AGS cells in the present study (Fig. 6*B*). Due to recent concerns regarding the specificity of this Ab, the ClC-3 protein expression was detected with three different anti-ClC-3 Abs. Figure 7*A* shows Western blot analysis of native ClC-3 expression in HeLa and AGS cells by using different anti-ClC-3 Abs as a primary Ab. A major band was detected for ClC-3 by using anti-ClC-3 Ab (Alomone Labs), corresponding to ~88 kDa, with several other bands at lower molecular masses in HeLa and AGS cells, indicating that Alomone Labs anti-ClC-3 Ab bind to many proteins in addition to ClC-3 and cannot be used as a specific probe of this protein under the conditions of our experiments. Control experiments using antigen-preabsorbed anti-ClC-3 Ab (Alomone Labs) confirmed the absence of these specific and nonspecific bands. Whereas only one band without any others was detected for ClC-3 by using anti-ClC-3 Ab (Santa Cruz Biotechnology) in HeLa and AGS cells. Figure 7*B* illustrates the effect of intracellular dialysis of 30 μg/ml anti-ClC-3 Ab (Santa Cruz Biotechnology) on $I_{Cl,swell}$ activated by hypotonic bath solutions over the voltage range of +100 to −100 mV at a holding potential of −60 mV. After 5 min of intracellular dialysis with this Ab, $I_{Cl,swell}$ was inhibited, and RVD was disrupted ($n = 7$, $P < 0.01$). The same results were obtained after intracellular dialysis of 7 μg/ml anti-ClC-3 Ab (the gift of Dr. Joseph R. Hume) shown as Fig. 7*C* ($n = 3$, $P < 0.01$). *I-V* in the presence of the different anti-ClC-3 Ab under isotonic or hypotonic bath solutions were shown in Fig. 7, *D* and *E*.

Figure 8 illustrates the changes in cell diameter after exposure to a hypoosmotic NMDG-Cl solution (250 mosM). The AGS cells without intracellular dialysis of anti-ClC-3 Ab had a mean relative cell diameter increase of 1.175 ± 0.00922 after exposure to hypotonic solutions for 10 min and an RVD to 1.08333 ± 0.00989 after exposure to hypotonic solutions for 14 min. In contrast, there was no subsequent RVD in the AGS cells dialyzed with anti-ClC-3 Ab, because the relative cell diameter after exposure to hypotonic solutions for

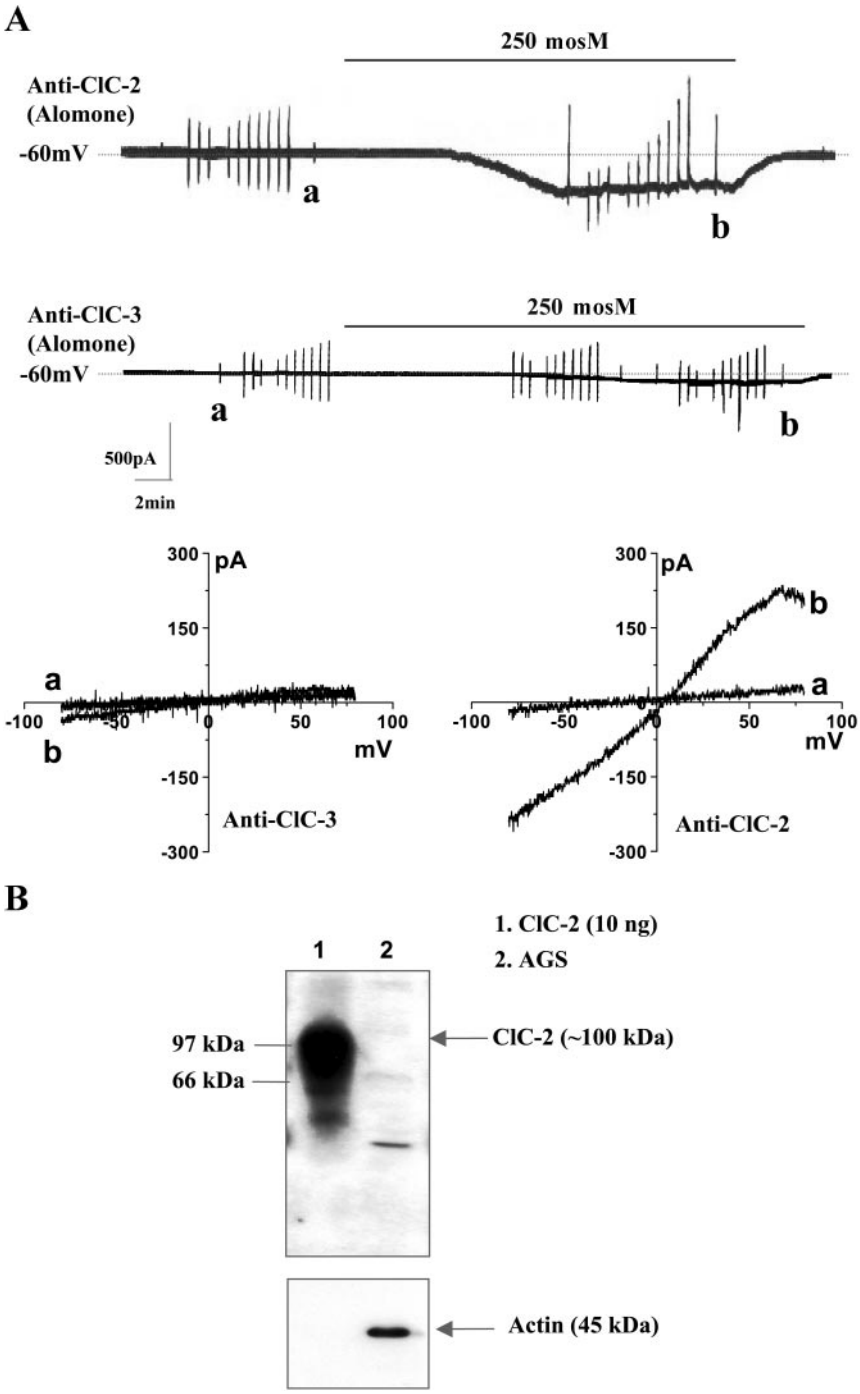

Fig. 6. Effect of intracellular dialysis of either ClC-2 antibody (Ab) or ClC-3 Ab on the Cl^- current activated by exposure to hypotonic solutions at a holding potential of −60 mV. *A*: *I-V* relationships were obtained from the current traces indicated at *a* and *b* ramp pulse, applied from −80 to +80 mV. *B*: Western blot analysis of native ClC-2 expression in AGS cells. Positive control (ClC-2 antigen, 10 ng) was detected, whereas ClC-2 was not found ($n = 5$). An actin band corresponding to ~45 kDa, was detected with anti-actin Ab suggesting that the proteins were intact in Western blot analysis. The ClC-2 protein is not present in AGS cells in the present study.

10 min remained elevated at 1.1992 ± 0.01968 (anti-ClC-3 Ab, $n = 6$; Santa Cruz Biotechnology) and 1.2275 ± 0.02056 ($C_{670–687}$ anti-ClC-3 Ab, $n = 4$), respectively. In addition, the latency of relative cell diameter increase of 10% was significantly decreased from 6.7 ± 0.6 min (control, $n = 6$) to 3.1 ± 0.5 min (anti-ClC-3, $n = 6$, Santa Cruz Biotechnology) and 3.4 ± 0.4 min (anti-ClC-3, $C_{670–687}$, $n = 4$), respectively ($P < 0.05$).

Molecular characterization. The RT-PCR technique was used to investigate the molecular expression of mRNA of the chloride channel ClC-3, MDR-1, and pICln (Fig. 9). With primers specific to the human cDNA sequences of ClC-3, bands corresponding to the expected fragment size, i.e., 540 bp, were obtained from RNA prepared from cultured human gastric epithelial cells. The PCR product was digested with *Eco*RI into two fragments of 320 and 220 bp as predicted. We also detected bands with fragment sizes of 600 and 726 bp with primers for MDR-1 and pICln, respectively. The PCR product of MDR-1 was digested into two fragments 384 and 216 bp as predicted. The PCR product of

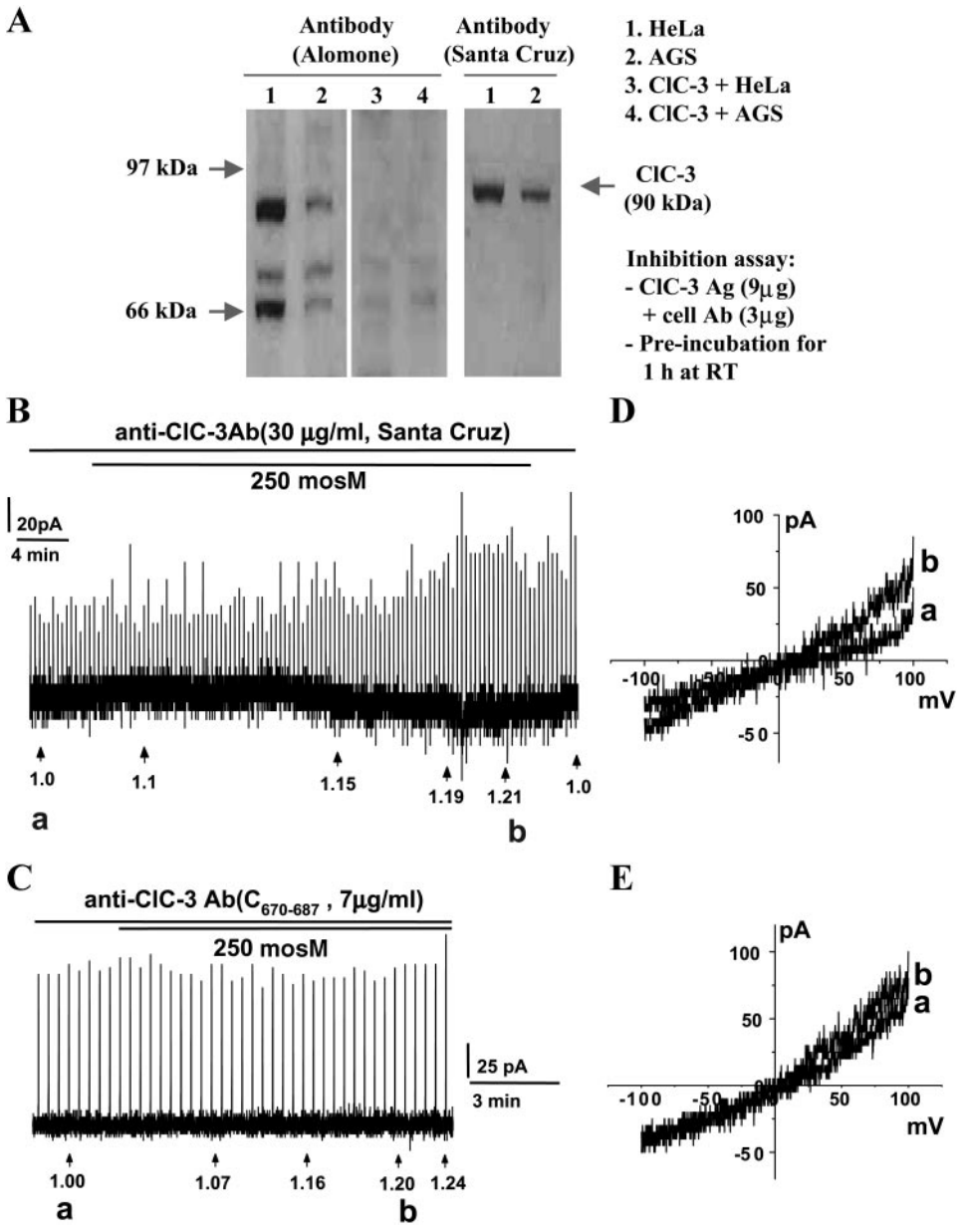

Fig. 7. The attenuation of native $I_{Cl,swell}$ after intracellular dialysis of specific anti-ClC-3 antibodies in AGS cells. *A*: Western blot analysis of native ClC-3 expression in AGS and HeLa cells. *B* and *C*: simultaneous measurement of relative cell diameter and membrane current after intracellular dialysis of anti-ClC-3 Ab (30 μg ml^{-1}; Santa Cruz Biotechnology) or another anti-ClC-3 Ab ($C_{670–687}$; 7 μg/ml). *D* and *E*: *I-V* relationships obtained from voltage ramp protocols (from +100 mV to −100 mV, $dV/dt = -0.20$ V/s) at different times as indicated in *B*(*a* and *b*) and *C*(*a* and *b*) in the presence of the different anti-ClC-3 Ab.

pICln was cloned into pGEM-T easy vector and identified as pICln with determining the nucleotide sequence.

DISCUSSION

With alterations in extracellular osmolarity, controlled efflux of chloride, potassium, and organic osmolytes occurs to compensate for changes in cell volume. Our present results suggest that human gastric epithelial cells possess Cl^- channels that are activated as the cells swell after exposure to hypotonic solution, which was demonstrated by the fact that *1*) the E_{rev}, which was close to the E_{rev} of chloride, shifted in expected direction when extracellular Cl^- concentrations were decreased from 86 to 46 and 16 mM; *2*) K^+ channel blocker TEA did not affect the current, and extracellular Na^+ replacement by NMDG did not influence this current, excluding the contamination of cationic (K^+ and Na^+) currents; *3*) changes of intracellular Ca^{2+} concentration from 0.1 to 1 or 10 mM did not affect the current significantly; and *4*) nonselective chloride channel blocker flufenamate, chloride transport blocker DIDS, the antioestrogen tamoxifen, and NPPB inhibited the hypotonicity-induced current significantly. The stilbene derivative Cl^- channel blocker DIDS, was reported to block the volume-sensitive Cl^- currents in epithelial Madin-Darby canine kidney cells and intestinal 407 cells (20), whereas DIDS does not block the cAMP-dependent Cl^- current related to the cystic fibrosis transmembrane conductance regulator (CFTR) gene (6), suggesting that the volume-sensitive Cl^- current in human gastric epithelial cells is not related to CFTR.

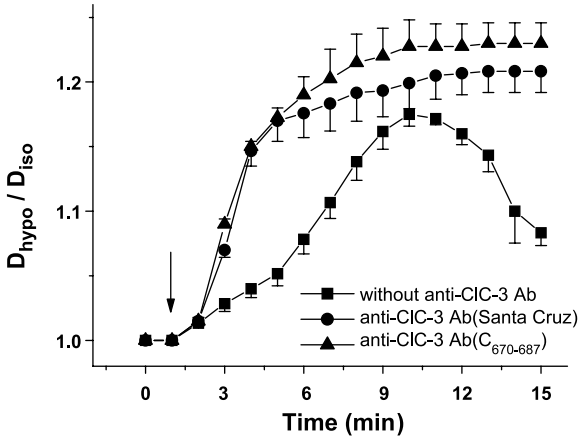

Fig. 8. Time course of relative cell diameter changes in single AGS cells in response to hypotonic bath solutions (250 mosM). Cells were bathed initially in a standard isotonic solution that was then switched to a hypotonic solution (arrow). The control AGS cells (■) swelled when exposed to a hypoosmotic NMDG-Cl solution. Subsequently, a regulatory decrease in cell diameter occurred. In contrast, the AGS cells dialyzed with anti-ClC-3 Ab (Santa Cruz Biotechnology, ●, $n = 6$) or anti-ClC-3 Ab ($C_{670-687}$, ▲, $n = 4$), although also swelling in response to hypotonic exposure, were unable to regulate cell diameter, suggesting that the AGS cells had an impaired regulatory volume decrease. Data were expressed as means ± SE.

To elucidate the molecular identity of volume-sensitive Cl^- channels, two candidate proteins (ClC-2 and ClC-3) have been discussed (9). ClC-2 contributes to physiological changes in membrane Cl^- permeability and cell volume homeostasis (19), which is known to have widespread tissue distribution with high mRNA levels in brain, kidney, heart, and liver and is activated by hypotonicity. It shows inward rectification and an anion selectivity of $Cl^- > Br^- > I^-$ (7, 23), different from our results (anion selectivity of $I^- > Br^- > Cl^- > F^-$ > gluconate), suggesting that the volume-sensitive Cl^- currents in human gastric epithelial cells are not mediated by a ClC-2 channel. In addition, in the present study, intracellular dialysis of ClC-2 Ab did not inhibit the current, and the absence of the ClC-2 protein in AGS cells, also supported this hypothesis.

The ClC-3 channel was first reported as a ubiquitously expressed protein, with high levels in brain, kidney, and lung (10). Duan et al. (3, 4) reported that the heterologous expression of ClC-3 in NIH/3T3 fibroblasts elicited a volume-activated chloride current with electrophysiological properties close to native chloride currents involved in RVD. Furthermore, antisense oligonucleotides (27) and anti-ClC-3 antibodies (5) were used to inhibit endogenous swelling-activated chloride currents and further supported the hypothesis that ClC-3 encodes a volume-activated chloride channel. Therefore, ClC-3 appeared to be the most likely candidate to encode a volume-activated chloride channel.

Although the role of ClC-3 as a volume-regulated chloride channel was controversial, it is still unknown if unexpected compensatory or redundancy mechanisms might be activated when a gene is missing (16), for example, the compensatory production of another channel similar to ClC-3 channel or other proteins including the second messengers (17). Importantly, the Alomone Labs Ab has been shown to bind to many proteins in addition to ClC-3 (22, 28) and cannot be used as a specific probe of this protein under the conditions of our experiments. So we used three different anti-ClC-3 Abs and verified that the volume-sensitive Cl^- current was inhibited and RVD was disrupted. Especially, the commercial anti-ClC-3 Ab (Santa Cruz Biotechnology) was selected, because only one band was detected for ClC-3 in Western blots, corresponding to ~88 kDa in HeLa and AGS cells, indicating that this Ab is specific to ClC-3. Intracellular dialysis with this Ab (Santa Cruz Biotechnology) into AGS cells abolishes or significantly attenuates native swelling-activated chloride channels function; whereas anti-ClC-2 Ab unaltered this function. The same results were obtained by using another specific anti-ClC-3 Ab (the gift of Dr. Joseph R. Hume, $C_{670-687}$), which was tested to be specific to ClC-3. The relative cell diameter of AGS cells dialyzed with either the commercial anti-ClC-3 Ab (Santa Cruz Biotechnology) or anti-ClC-3 ($C_{670-687}$) Ab increased more rapidly in hypotonic solution than that of control AGS cells. This suggests that the anti-ClC-3 Abs used in our study exhibited strong reactivity across species for ClC-3. Thus our data provide strong evidence that endogenous ClC-3 is a major molecular component responsible for the volume-sensitive Cl^- current in human gastric epithelial cells, consistent with previous studies (3, 5). Site-directed mutagenesis experiments (3, 4) and ClC-3 antisense experiment also support the hypothesis (8, 27).

However, we cannot exclude the possibility that the endogenous ClC-3 may also act as a channel regulator, or it may cooperate with other proteins, for example pICln and P-gp, to form a complex that contributes to the modulation of, or constitutes, the volume-activated chloride current. When one of the proteins in the system is inhibited, then it is more difficult to activate the

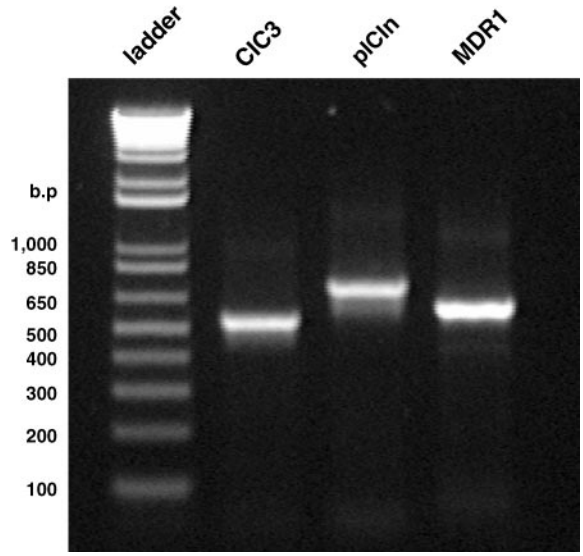

Fig. 9. RT-PCR analysis of ClC-3, pICln, and multidrug resistance gene (MDR1) mRNA expression in AGS cells.

volume-sensitive current. The detection of ClC-3 mRNA and ClC-3 channel regulators pICln and P-gp in human gastric epithelial cells also support the possibility.

In conclusion, in human gastric epithelial cells, a Ca^{2+}-independent, volume-sensitive chloride current is present. Reduction in $I_{Cl,swell}$ density and the disruption of RVD after intracellular dialysis of anti-ClC-3 antibodies in AGS cells, although anti-ClC-2 Ab failed to significantly affect them in the present study, strongly supports a fundamental role of endogenous ClC-3 in native swelling-activated chloride channels function and cell volume regulation in human gastric epithelial cells.

Present address of N. G. Jin: Department of Physiology, Yanbian University, College of Medicine, Yanji 133000, China.

DISCLOSURES

This work was supported by a grant of the Korea Health 21 Research and Development Project, Ministry of Health and Welfare, Republic of Korea (HMP-00-CH-02-0002) and Year 2001 BK21 Project for Medicine, Dentistry, and Pharmacy.

REFERENCES

1. **Bond TD, Ambikapathy S, Mohammad S, and Valverde MA.** Osmosensitive Cl^- currents and their relevance to regulatory volume decrease in human intestinal T84 cells: outwardly vs. inwardly rectifying currents. *J Physiol* 511: 45–54, 1998.
2. **Bond TD, Valverde MA, and Higgins CF.** Protein kinase C phosphorylation disengages human and mouse-1a P-glycoproteins from influencing the rate of activation of swelling-activated chloride currents. *J Physiol* 508: 333–340, 1998.
3. **Duan D, Cowley S, Horowitz B, and Hume JR.** A serine residue in ClC-3 links phosphorylation-dephosphorylation to chloride channel regulation by cell volume. *J Gen Physiol* 113: 57–70, 1999.
4. **Duan D, Winter C, Cowley S, Hume JR, and Horowitz B.** Molecular identification of a volume-regulated chloride channel. *Nature* 390: 417–421, 1997.
5. **Duan DY, Zhong JM, Hermoso M, Satterwhite CM, Rossow CF, Hatton WJ, Yamboliev I, Horowitz B, and Hume JR.** Functional inhibition of native volume-sensitive outwardly rectifying anion channels in muscle cells and xenopus oocytes by anti-ClC-3 antibody. *J Physiol* 531: 437–444, 2001.
6. **Gray MA, Plant S, and Argent BE.** cAMP-regulated whole cell chloride currents in pancreatic duct cells. *Am J Physiol Cell Physiol* 264: C591–C602, 1993.
7. **Grunder S, Thiemann A, Pusch M, and Jentsch TJ.** Regions involved in the opening of CIC-2 chloride channel by voltage and cell volume. *Nature* 360: 759–762, 1992.
8. **Hermoso M, Satterwhite CM, Andrade Y, Hidalgo J, Wilson SM, Horowitz B, and Hume JR.** ClC-3 is a fundamental molecular component of volume-sensitive outwardly rectifying Cl^- channels and volume regulation in HeLa cells and *Xenopus laevis* oocytes. *J Biol Chem* 277: 40066–40074, 2002.
9. **Hoffmann EK.** Intracellular signaling involved in volume regulatory decrease. *Cell Physiol Biochem* 10: 273–288, 2000.
10. **Huang P, Liu J, Di A, Robinson NC, Musch MW, Kaetzel MA, and Nelson DJ.** Regulation of human CLC-3 channels by multifunctional Ca^{2+}/calmodulin-dependent protein kinase. *J Biol Chem* 276: 20093–20100, 2001.
11. **Jordt SE and Jentsch TJ.** Molecular dissection of gating in the ClC-2 chloride channel. *EMBO J* 16: 1582–1592, 1997.
12. **Kim JM, Kim JS, Jung HC, Song IS, and Kim CY.** Up-regulation of inducible nitric oxide synthase and nitric oxide in *Helicobacter pylori*-infected human gastric epithelial cells: possible role of interferon-γ in polarized nitric oxide secretion. *Helicobacter* 7: 116–128, 2002.
13. **Krapivinsky GB, Ackerman MJ, Gordon EA, Krapivinsky LD, and Clapham DE.** Molecular characterization of a swelling-induced chloride conductance regulatory protein, pICln. *Cell* 76: 439–448, 1994.
14. **Lang F, Busch GL, Ritter M, Volkl H, Waldegger S, Gulbins E, and Haussinger D.** Functional significance of cell volume regulatory mechanisms. *Physiol Rev* 78: 247–306, 1998.
15. **Li X, Shimada K, Showalter LA, and Weinman SA.** Biophysical properties of ClC-3 differentiate it from swelling-activated chloride channels in Chinese hamster ovary-K1 cells. *J Biol Chem* 275: 35994–35998, 2000.
16. **Nehrke K, Arreola J, Nguyen HV, Pilato J, Richardson L, Okunade G, Baggs R, Shull GE, and Melvin JE.** Loss of hyperpolarization-activated Cl^- current in salivary acinar cells from Clcn2 knockout mice. *J Biol Chem* 277: 23604–23611, 2002.
17. **Nilius B, Eggermont J, Voets T, Buyse G, Manolopoulos V, and Droogmans G.** Properties of volume-regulated anion channels in mammalian cells. *Prog Biophys Mol Biol* 68: 69–119, 1997.
18. **Paulmichl M, Li Y, Wickman K, Ackerman M, Peralta E, and Clapham D.** New mammalian chloride channel identified by expression cloning. *Nature* 356: 238–241, 1992.
19. **Roman RM, Roderic LS, Andrew PF, Gerald HC, Doctor RB, and Fitz JG.** ClC-2 chloride channels contribute to HTC cell volume homeostasis. *Am J Physiol Gastrointest Liver Physiol* 280: G344–G353, 2001.
20. **Rothstein A and Mack I.** Volume-activated K^+ and Cl^- pathways of dissociated epithelial cells (MDCK): role of Ca^{2+}. *Am J Physiol Cell Physiol* 258: C827–C834, 1990.
21. **Shimada K, Li X, Xu G, Nowak DE, Schowalter LA, and Weinman SA.** Expression and canalicular localization of two isoforms of the ClC-3 chloride channel from rat hepatocytes. *Am J Physiol Gastrointest Liver Physiol* 279: G268–G276, 2000.
22. **Stobrawa SM, Breiderhoff T, Takamori S, Engel D, Schweizer M, Zdebik AA, Bösl MR, Ruether K, Jahn H, Draguhn A, Jahn R, and Jentsch TJ.** Disruption of ClC-3, a chloride channel expressed on synaptic vesicles, leads to a loss of the hippocampus. *Neuron* 29: 185–196, 2001.
23. **Thiemann A, Gründer S, Pusch M, and Jentsch TJ.** A chloride channel widely expressed in epithelial and non-epithelial cells. *Nature* 356: 57–60, 1992.
24. **Valverde MA, Bond TD, Hardy SP, Taylor JC, Higgins CF, Altamirano J, and Alvarez-Leefmans FJ.** The multidrug resistance P-glycoprotein modulates cell regulatory volume decrease. *EMBO J* 15: 4460–4468, 1996.
25. **Vanoye CG, Altenberg GA, and Reuss L.** P-glycoprotein is not a swelling-activated Cl^- channel: possible role as a Cl^- channel regulator. *J Physiol* 502: 249–258, 1997.
26. **Waldegger S, Steuer S, Risler T, Heidland A, Capasso G, Massry S, and Lang F.** Mechanisms and clinical significance of cell volume regulation. *Nephrol Dial Transplant* 13: 867–874, 1998.
27. **Wang LW, Chen LX, and Jacob TJC.** The role of ClC-3 in volume-activated chloride currents and volume regulation in bovine epithelial cells demonstrated by antisense inhibition. *J Physiol* 524: 63–75, 2000.
28. **Weylandt KH, Valverde MA, Nobles M, Raguz S, Amey JS, Diaz M, Nastrucci C, Higgins CF, and Sardini A.** Human ClC-3 is not the swelling-activated chloride channel involved in cell volume regulation. *J Biol Chem* 276: 17461–17467, 2001.
29. **Xiong H, Li C, Garami E, Wang Y, Ramjeesingh M, Galley K, and Bear CE.** ClC-2 activation modulates regulatory volume decrease. *J Membr Biol* 167: 215–221, 1999.
30. **Xu WX, Kim SJ, So I, Kang TM, Rhee JC, and Kim KW.** Volume-sensitive chloride current activated by hyposmotic swelling in antral gastric myocytes of the guinea-pig. *Pflügers Arch* 435: 9–19, 1997.